Available online at www.sciencedirect.com
ScienceDirect
Bioorganic Chemistry 35 (2007) 444–457
BIOORGANIC CHEMISTRY
www.elsevier.com/locate/bioorg

Quantum chemical modeling of enzymatic reactions: The case of 4-oxalocrotonate tautomerase

Robin Sevastik, Fahmi Himo *

Department of Theoretical Chemistry, School of Biotechnology, Royal Institute of Technology, AlbaNova University Center, SE-106 91 Stockholm, Sweden

Received 4 August 2007
Available online 27 September 2007

Abstract

The reaction mechanism of 4-oxalocrotonate tautomerase (4-OT) is studied using the density functional theory method B3LYP. This enzyme catalyzes the isomerisation of unconjugated α-keto acids to their conjugated isomers. Two different quantum chemical models of the active site are devised and the potential energy curves for the reaction are computed. The calculations support the proposed reaction mechanism in which Pro-1 acts as a base to shuttle a proton from the C3 to the C5 position of the substrate. The first step (proton transfer from C3 to proline) is shown to be the rate-limiting step. The energy of the charge-separated intermediate (protonated proline-deprotonated substrate) is calculated to be quite low, in accordance with measured pK_a values. The results of the two models are used to evaluate the methodology employed in modeling enzyme active sites using quantum chemical cluster models.

Keywords: 4-Oxalocrotonate tautomerase; Density functional theory; Reaction mechanism

1. Introduction

4-Oxalocrotonate tautomerase (4-OT) is a bacterial enzyme that catalyzes the isomerisation of unconjugated α-keto acids to their conjugated isomers (Scheme 1). It is a part of

* Corresponding author.
E-mail address: himo@theochem.kth.se (F. Himo).

0045-2068/$ - see front matter © 2007 Elsevier Inc. All rights reserved.
doi:10.1016/j.bioorg.2007.08.003

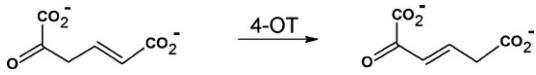

Scheme 1. Reaction catalyzed by 4-oxalocrotonate tautomerase.

a degradation pathway that converts diverse aromatic hydrocarbons to intermediates in the citric acid cycle (Krebs cycle) in the soil bacterium *Pseudomonas putida mt-2* [1,2].

4-OT is a homo-hexamer composed of a trimer of dimers, with 62 amino acids per monomer [3]. The crystal structure showed that the six active sites are located at the dimer interfaces [4,5]. Based on experimental [6–11] and theoretical [12–15] studies, a generally accepted mechanism for 4-OT has emerged and is presented in Scheme 2. The conserved terminal proline (Pro-1) acts as a general base, abstracting a proton from the C3 position and delivering it back to the C5 position. The pK_a of this proline has been measured to ~6.4, c:a 3 units lower than for proline in solution [9], which indicates that it is largely deprotonated under physiological conditions and can thus act as the general base. The k_{cat} value has been measured to be 3500 s^{-1} [11], which, using classical transition state theory, can be converted to a rate-limiting barrier of c:a 13 kcal/mol. From crystallographic [4,5] and mutational studies [16–18], three arginine residues have been identified as important for the reaction. Arg-61′ and Arg-11′ bind the carboxylate groups of the substrate, while Arg-39″ contributes to the catalysis by forming a hydrogen bond to the carbonyl oxygen

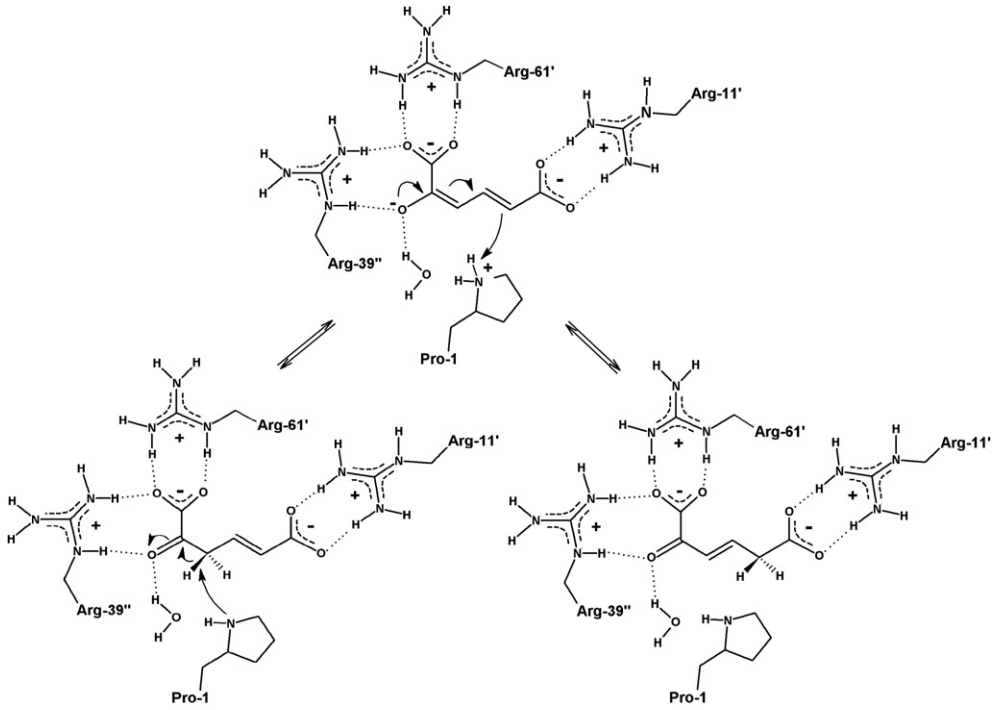

Scheme 2. Proposed reaction mechanism of 4-OT.

of the substrate, hence stabilizing the negative charge that forms in the transition states and intermediate. Arg-11′ has also been suggested to be important for catalysis, by acting as an electron sink, drawing electrons to the C5 position and facilitating protonation in the second step of the reaction [19]. Mutation of Arg-39″ to the non-coded isosteric citrulline by chemical synthesis techniques showed that the electrostatic stabilization provided by the positive charge is responsible for lowering of the barrier [18]. This has, however, been questioned by recent molecular dynamics and quantum mechanical/molecular mechanical (QM/MM) simulations [20].

The reaction mechanism of 4-OT has previously been investigated by Cisneros et al. using QM/MM techniques [13]. The QM part (treated at the B3LYP/6-31G*//HF/3-21G level of theory) consisted of the substrate, the proline, and an ordered water molecule, while the rest of the enzyme was treated using MM. This study ruled out the possibility of a participation of a general acid in the reaction. The potential energy surface obtained using this approach yielded a barrier of 14.5 kcal/mol for the first step. The intermediate was found to lie in a shallow minimum, 13.5 kcal/mol higher than the reactant and only 2.9 kcal/mol below the second transition state, which is the delivery of the proton to the C5 position. Subsequent investigations using the same methods [14,15] gave somewhat lower barriers, and also considered the possibility that it is the enol form of the substrate (i.e., 2-hydroxymuconate) that reacts with the 4-OT enzyme. The calculated rate-limiting barriers were shown to slightly favor the reaction of the enol form of the substrate over the keto-form [15].

Very recently, Tuttle and Thiel also used QM/MM methods to investigate the same reaction [21]. The QM part was treated at the BLYP/TZVPP level of theory and consisted of the substrate and the proline residue. The barriers were calculated to be considerably higher (29.1 and 29.6 kcal/mol for the first and second steps, respectively) and also the energy of the intermediate was very high (+26.5 kcal/mol). Using the same geometries but extending the QM part to also include the three important arginine residues (energies calculated as single points), resulted only in a modest lowering of the barriers. However, when the system was re-equilibrated starting from the optimized structure of the intermediate, with the QM part frozen, the barriers were found to be considerably lower and the side chain of Arg-39″ rotated to bind the substrate differently [21].

In recent years, many researchers have applied quantum chemical methods to make relatively small models of enzyme active sites and study their reaction mechanisms [22]. The rest of the enzyme is usually treated using a homogenous polarizable medium with some dielectric constant. The method of choice is the Density Functional Theory (DFT) approach, and in particular the B3LYP functional [23]. The calculated energies can often be sufficient to substantiate or rule out a suggested reaction mechanism. The general experience has been that a well-chosen quantum model can reproduce the chemistry that takes place in an enzyme active site to such a high degree that it can be helpful in answering mechanistic questions. This methodology has been applied to a wide spectrum of enzymes, often with great success [22]. In this context, the reaction mechanism of the 4-OT enzyme represents a very interesting case to test such methodology. The charge separation in the intermediate state is a particularly challenging feature, which a small quantum chemical approach could have difficulties treating.

In the present study, we investigate the energetics of this enzyme using two active site models consisting of 77 and 177 atoms. The aim is to examine how well the active site models work and to shed more light on the specific reaction mechanism of 4-OT.

2. Computational details

All geometries and energies presented in this study are computed using the B3LYP [23] density functional theory method as implemented in the Gaussian03 program package [24]. Geometry optimizations were performed using the 6-31G(d,p) basis set. Based on these geometries, single point calculations with the larger basis set 6-311+G(2d,2p) were done to obtain more accurate energies. Solvation energies were added as single point calculations using the conductor-like solvation model CPCM [25] at the B3LYP/6-31G(d,p) level. In this model, a cavity around the system is surrounded by a polarizable dielectric continuum. Several dielectric constants ($\varepsilon = 2$, 4, 8, 16, and 80) were used to model the environment.

Hessians were calculated at the B3LYP/6-31G(d,p) level to confirm the nature of the stationary points, with no negative eigenvalues for minima and only one negative eigenvalue for transition states. The Hessians were also used to calculate zero-point vibrational effects. The size of the large model (Model B, see below) prohibited the calculation of Hessians for this model, so the zero-point vibrational effects were taken from the frequency calculations of the smaller Model A. In the models, some centers were kept fixed to their X-ray positions in the geometry optimization. This procedure gives rise to a few small imaginary frequencies, typically on the order of 10–30i cm^{-1}. These frequencies do not contribute significantly to the zero-point energies and can thus be tolerated.

3. Results

Two quantum chemical models of the active site of 4-OT were prepared. Model A consists of 77 atoms and contains the substrate, models of Pro-1 and the three arginine residues, and two water molecules. To test the validity and reliability of the results of Model A, we devised a quite large model consisting of 177 atoms (Model B), in which several additional groups of the active site were included.

3.1. Model A

A relatively small model of the active site was built based on the crystal structure of 4-OT from *Pseudomonas putida mt-2* (PDB code 4OTA [5]). This model includes the 2-oxo-4-hexenedioate substrate, the catalytic proline residue (Pro-1), the three arginines (Arg-39″, Arg-61′, Arg-11′), and two structural water molecules (W1 and W2) (see Fig. 1).

In the crystal structure, the substrate-binding cavity (as defined by the arginine residues and the proline) is too large for the substrate, i.e., these residues are too far away from each other to properly bind the substrate. To get a proper docking, the substrate was first placed manually in the active site and the entire lengths of the active site residues were kept in the model, with the outermost atoms locked to their crystallographic positions. A geometry optimization was then performed at a low level of theory (HF/3-21G) and the groups moved closer to bind the substrate. The long chains of the arginines were then truncated at the C_δ positions and a geometry optimization at the B3LYP/6-31G(d,p) was performed with these positions locked. To prevent the arginine groups from rotating in an undesired fashion, two nitrogen atoms of Arg-39″ and Arg-61′ were also kept fixed (as indicated by arrows in the figures). The total number of atoms in the model is 77 and the total charge is

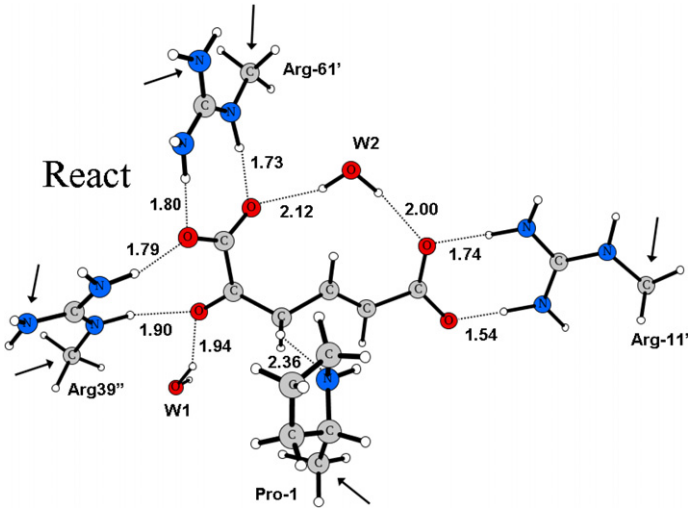

Fig. 1. Optimized reactant structure of Model A. Distances are in angstrom (Å). Arrows indicate centers that are fixed to their crystallographic positions during geometry optimization.

+1. The result of this procedure (displayed in Fig. 1) constitutes the reactant structure, relative to which all the energies will be compared.

We first note that the three positively charged arginines bind the substrate quite nicely, with two hydrogen bonds each. W2 forms two hydrogen bonds to the two carboxylates of the substrate, while W1 forms a hydrogen bond to the carbonyl oxygen of the substrate.

The first step of the suggested 4-OT reaction mechanism is the proton transfer from the C3 carbon of the substrate to the N1 nitrogen of Pro-1 (Scheme 2). As seen from Fig. 1, the proline nitrogen in this model is in a perfect position to accept a proton from the substrate, with an H–N distance of 2.36 Å.

We have managed to locate the transition state for this reaction step (TS1). The optimized TS1 structure and the resulting intermediate structure (Inter) are shown in Fig. 2. At the transition state, the critical C3-H and H–N distances are 1.47 and 1.29 Å, respectively. Without inclusion of solvation effects, the barrier is calculated to be 12.8 kcal/mol and the intermediate is calculated to lie at +9.8 kcal/mol relative to the reactant.

It is interesting to monitor some geometrical changes that take place in going from the reactant to the intermediate. The hydrogen bond distance between Arg-39″ and the C2 oxygen of the substrate decreased from 1.90 Å to 1.70 Å. A similar change was observed for the hydrogen bond to W1, from 1.94 Å to 1.70 Å. These changes are results of the negative charge that develops at the carbonyl oxygen in the intermediate structure and show that the role of Arg-39″ and W1 is to stabilize this charge formation, thereby lowering the energy barrier for the proton transfer.

An approximate way to estimate the energetic effects of the parts of the enzyme that are not included in the quantum chemical model is to assume that the surrounding is a homogenous polarizable medium with some assumed dielectric constant ε. This approximation has been used frequently in conjunction with quantum chemical models of the enzyme active sites [22]. The choice of the dielectric constant is somewhat arbitrary, but the value $\varepsilon = 4$ is frequently used in similar studies. In the present study, we chose to use a number

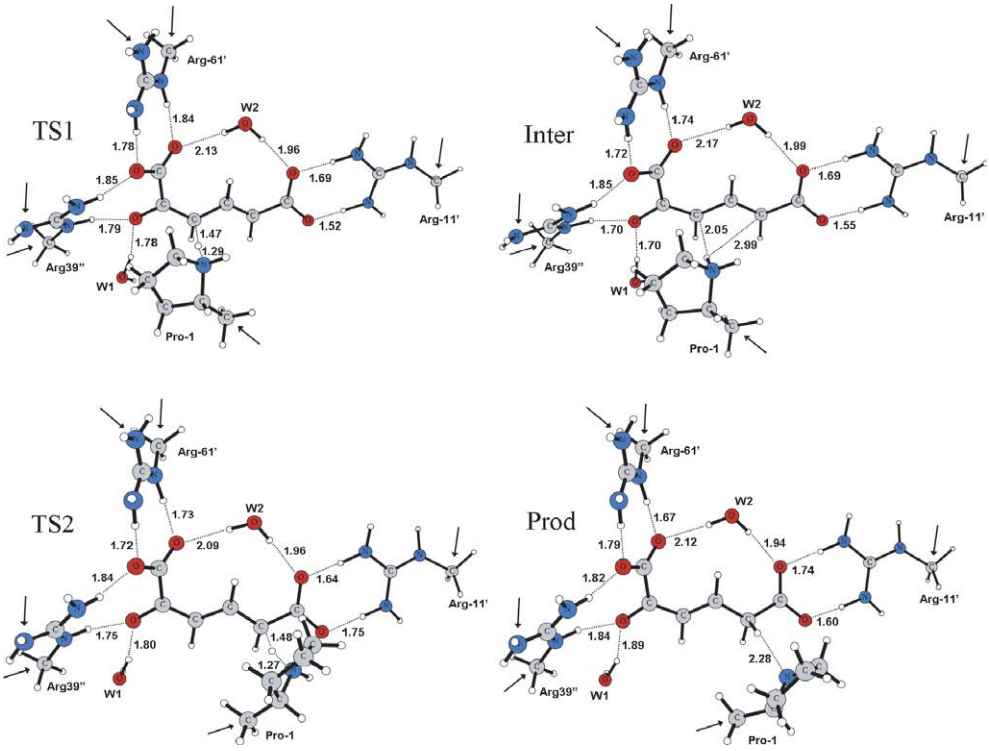

Fig. 2. Optimized structures of TS1, Inter, TS2, and Prod of Model A.

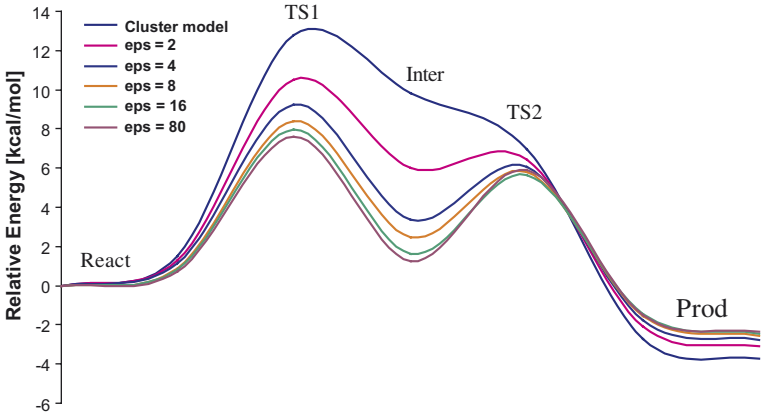

Fig. 3. Potential energy curves obtained for Model A.

of different dielectric constants ($\varepsilon = 2$, 4, 8, 16, and 80) to investigate the influence of the choice on the energetics. The results of this procedure are shown in Fig. 3.

As expected, solvation effects lower the energies of both TS1 and the intermediate compared to the reactant. Using $\varepsilon = 4$, for example, the barrier is decreased from 12.8 to

9.2 kcal/mol, and the energy of the intermediate is lowered from 9.8 to 3.4 kcal/mol. It is easy to rationalize these results considering that the reaction step under study is a proton transfer that results in a positive charge on the proline and an additional negative charge on the substrate. Solvation of the transition state and intermediate lowers the energy of the charge-separated complex compared to the reactant species.

The second step of the reaction is the transfer of the proton back from the proline to the C5 carbon of the substrate. We have calculated the transition state (TS2) for this step (optimized structure shown in Fig. 2). It turns out that the transition state in the cluster model (without the inclusion of solvation effects and after the basis set correction) has an energy that is 2.8 kcal/mol lower than the intermediate (i.e., +7.0 kcal/mol relative to the reactant). This is of course an artifact of the small model, which lacks proper solvation of the charge-separated intermediate. When dielectric solvation is applied, the intermediate energy is lowered compared to TS2 and a proper barrier is obtained. For $\varepsilon = 4$, for example, the energy of TS2 is 2.7 kcal/mol higher than the intermediate. At TS2, the N–H and H-C5 bond distances are 1.27 Å and 1.48 Å, respectively. These distances are almost identical to the corresponding distances in TS1.

The final product in this model (Fig. 2) is calculated to have an energy of −3.7 kcal/mol compared to the reactant. This value is quite independent of the applied solvation. The potential energy curves for the full reaction are presented in Fig. 3.

3.2. Model B

A considerably larger model (called Model B) that consists of 177 atoms was constructed to investigate the validity of the results presented above. The following parts were added to Model A: the side chain of Phe-50′ and the backbone chains of Ile-7′, Leu-8′, Ser-37, and Ile-27. All these groups help orienting the proline and the substrate within the

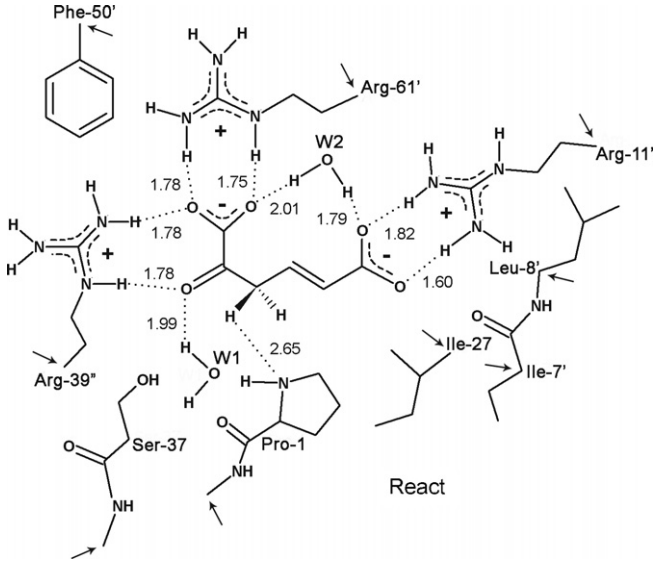

Fig. 4. Schematic figure showing the groups included in Model B. Selected optimized distances of the reactant species are shown.

active site and provide solvation to the charges that are developing during the reaction. In addition, the side chains of Arg-39″, Arg-61′, Arg-11′, and Pro-1 are longer than in Model A, to grant more flexibility to these groups. Also in this model, certain atoms were kept fixed in order to maintain the structure close to the X-ray structure. These positions are indicated by arrows in Fig. 4.

A problem that immediately emerges when quantum chemical models of this size are used is that different stationary points can lie in different local minima, giving rise to unreliable energy differences. In the present calculations, we have by visual inspection and alignment of structures done our best to confirm that the parts that do not directly participate in the reaction are in the same local minima. A schematic drawing of the reactant species of Model B is displayed in Fig. 4 (a ball-and-stick picture of a model of this size is too crowded to be meaningful). The basic features of the core region (substrate, arginines, and proline) are very similar to Model A. As before, the proline nitrogen is in good position to accept the proton from the substrate, with an H–N distance is 2.65 Å.

Similarly to Model A, we have optimized all stationary points (React, TS1, Inter, TS2, and Prod) for this model. Important structural parameters are shown in Fig. 5 and the resulting potential energy curves are presented in Fig. 6. We first note that structural parameters in general do not differ much from those obtained for Model A. However, some critical parameters change somewhat. For example, the critical C3-H and H–N distances at TS1 are 1.32 Å and 1.44 Å, respectively, compared to 1.47 Å and 1.29 Å, respectively, for Model A, indicating an earlier transition state in Model B compared to Model A. On the other hand, TS2 seems to be later in Model B compared to Model A. The N–H

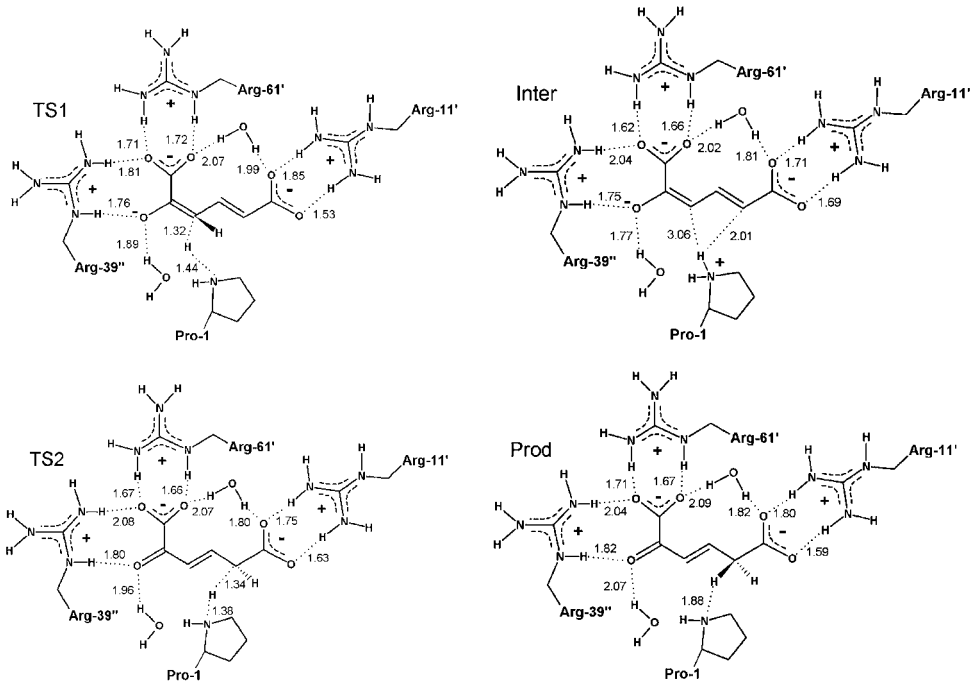

Fig. 5. Schematic representation of important optimized bond distances of TS1, Inter, TS2, and Prod of Model B.

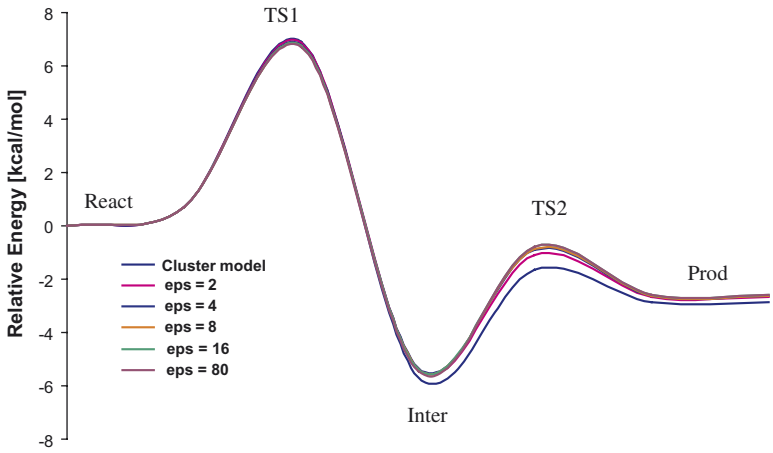

Fig. 6. Potential energy curves obtained for Model B.

and H-C5 distances are 1.38 Å and 1.34 Å, respectively (compared to 1.27 Å and 1.48 Å, respectively, in Model A). These geometries reflect the fact that the energy of the intermediate is lower in Model B compared to Model A. Indeed, the intermediate in Model B is calculated to be 5.7 kcal/mol lower than the reactant, which results in a lower TS1, calculated to lie at +6.9 kcal/mol. TS2 is 4.0 kcal/mol higher than the intermediate and the final product is 2.9 kcal/mol lower than the reactant.

The energy of the intermediate is thus lower now in the larger model compared to the small model. The specific solvation that is added in the model in the form of explicit groups around the substrate and proline results in an additional stabilization of c:a 7 kcal/mol compared to the homogenous solvation of Model A ($\varepsilon = 80$).

A very important feature of the potential energy curves obtained for Model B (Fig. 6) is that inclusion of solvation effects, in the form of homogenous polarizable medium on top of the quantum chemical cluster model, now changes the energies very modestly. This is because most of the solvation of the substrate and the proline (the critical parts that are changing charge states) is already included explicitly in the quantum model.

4. Mutation of Arg39″

As mentioned in the Introduction, mutation of the Arg-39″ residue to the non-coded isosteric citrulline by chemical synthesis techniques resulted in a 1600-fold decrease of k_{cat}

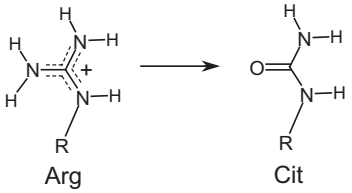

Scheme 3. Arginine to Citrulline mutation.

[18]. Because the citrulline lacks the positive charge of arginine (Scheme 3), this result was interpreted such that the Arg-39″ provides electrostatic stabilization to the developing charge of the enolate, thereby lowering of the barrier [18]. Interestingly, earlier Arg-39″ to Alanine mutation experiments resulted in a 125-fold decrease of k_{cat} [16]. This indicates that an active site water molecule (expected to be replace the guanidinium side chain in the Arg39Ala mutant) provides slightly more stabilization to the charged enolate intermediate compared to the neutral urea moiety of citrulline [18].

A recent molecular dynamics and QM/MM study by Tuttle et al. has questioned these conclusions [20]. Instead, the effect was proposed to arise from a distortion of the active site, which alters the positioning of the substrate. However, no energies were reported in this study.

We were interested in resolving this issue and finding out whether our models can be used in this kind of mutational studies. Accordingly, Models A and B were altered such that the Arg-39″ was mutated into Cit (=NH_2^+ group was replaced by =O). The React and TS1 were re-optimized and their energies were calculated. Also here, we chose to use several dielectric constants to investigate the influence of the choice on the energetics. The optimized structures are displayed in Fig. 7 and the calculated reaction barriers are shown in Fig. 8.

The main structural differences compared to the ''wild-type'' geometries (Figs. 1 and 4) are the hydrogen bonding distances of the Cit to the substrate. Due to the lack of the positive charge in citrulline, the hydrogen bond distances of this residue to the substrate are

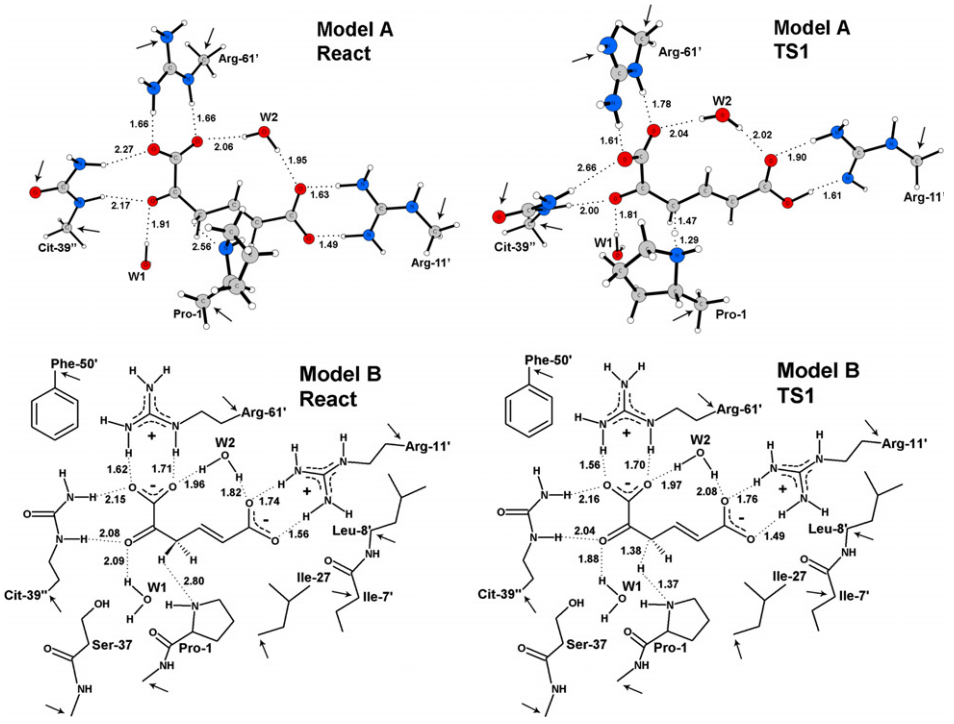

Fig. 7. Optimized geometries of Arg39Cit mutant models.

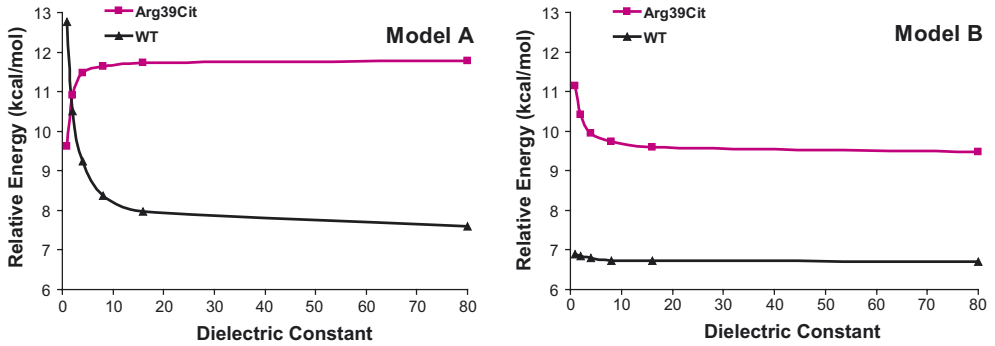

Fig. 8. Calculated energy barriers for the first step of the 4-OT reaction for wild-type and Arg39Cit mutant models.

now considerably longer, in the range of 0.3–0.5 Å. As a result of this, the hydrogen bonds to the two other arginines (Arg-61′ and Arg-11′) are shorter in the mutant.

At the transition state, the same trend is present. However, in the small Model A, the high concentration of charge developing on the substrate at the transition state, and the relative smallness of the model causes a proton to transfer from the positively charged Arg-11′ to the carboxylate of the substrate. This is not seen in the much larger Model B, where enough surrounding is included in the quantum model to stabilize the emerging charge on the substrate without transferring a proton.

The calculated activation barriers as functions of the dielectric constant are displayed in Fig. 8 for both the mutants and the wild-type models. The experimentally measured 1600-fold decrease in k_{cat} corresponds to a barrier increase of ca 4 kcal/mol (as calculated using classical transition state theory). As seen from Fig. 8, both Model A and Model B reproduce this increase quite nicely.

The small Model A gives the wrong trend in the cluster calculation, i.e., the Arg39Cit mutant has a lower barrier than the wild-type. However, application of dielectric solvation immediately reverses the trend. With $\varepsilon = 4$, the calculated barrier difference between the mutant and wild-type is 2.2 kcal/mol, and with $\varepsilon = 80$ it is 4.2 kcal/mol, in very good agreement with the experimental result. The larger Model B yields the correct trend already at the cluster model ($\Delta E = 4.3$ kcal/mol). Application of dielectric solvation decreases this values somewhat, to 3.2 and 2.8 kcal/mol, using $\varepsilon = 4$ and $\varepsilon = 80$, respectively.

These results indicate that the effect of the Arg39Cit mutation is of electrostatic nature, as suggested originally by Metanis et al. [18], and that the models indeed can be used for this kind of investigations.

5. Discussion and conclusions

In the present paper, two quantum chemical models of different sizes were employed to investigate the reaction mechanism of the 4-oxalocrotonate tautomerase enzyme. The conclusions can be divided into two parts, one related to the specific reaction under study, i.e., the 4-OT reaction mechanism, and one related to the methodology used.

The calculations presented here give strong support to the proposed reaction mechanism in which Pro-1 acts as a base to shuttle a proton from the C3 to the C5 position of the substrate (Scheme 2). The reaction was found to proceed with plausible barriers without the assistance of a general acid, as previously found by Cisneros et al. [13]. The Arg-39″ residue and the water molecule W1 are sufficient to stabilize the negative charge that develops on the substrate in the transition states and the intermediate structure.

However, the quantum chemical models employed in the current study yield potential energy curves (Figs. 3 and 6) that are qualitatively different from those obtained by previous QM/MM calculations [13,21]. From our calculations it is clear that the first step (the first proton transfer from C3 to the proline) is the rate-limiting step, whereas the QM/MM calculations yield similar barriers for both steps, or even predict the second step to be slightly higher [13,15,21]. Furthermore, our calculations predict that the energy of the charge-separated intermediate is quite low, +3.4 kcal/mol for the small model (using $\varepsilon = 4$ solvation), and −5.7 kcal/mol for the large model. Because the considered reaction step is a proton transfer, the energy difference can advantageously be compared to experimental relative acidities of the species involved. The pK_a of the active site proline has been experimentally determined to 6.4, which is c:a 3 U lower than for proline in solution [9]. The pK_a of the substrate has been measured experimentally to be 10.5 [18b]. Binding of the substrate to the 4-OT active site is expected to lower this value, because of the stabilizing effect of the active site surrounding, mainly the positively-charged Arg-39″ group. This suggests that the pK_a values of the two groups are relatively close to each other, which means that the energy of the intermediate is close to the energy of the reactant, in very good agreement with the results of our quantum chemical Models A and B.

Moreover, the calculations presented in the current paper demonstrate that the decease in k_{cat} caused by mutation of Arg39″ into the neutral citrulline is due to loss of electrostatic stabilization of the transition state of the first rate-limiting proton transfer. Our theoretical mutation calculations give a barrier raise that is in excellent agreement with the experimentally determined decrease in k_{cat}. These results are in disagreement with the QM/MM calculations of Tuttle et al., which predicted the mutation to cause the k_{cat} decrease by distorting the active site [20].

Due to the charge separation in the intermediate, the 4-OT reaction is particularly challenging to model using small active site models, and represents hence an interesting case to test the methodology. Unless the model is carefully chosen and the surrounding is properly accounted for, small models will yield unrealistic energies.

By comparing the results of Model A to those of Model B (Figs. 3 and 6), one can conclude that a relatively small, but carefully chosen, model of the enzyme active site, in conjunction with implicit solvent models can be very useful in studying enzyme reaction mechanism. The general trends of the potential energy curve are reproduced, but because of the high degree of charge separation, the continuum solvation is not expected to yield very accurate energies. The energies of the charge-separated species (TS1, intermediate, and TS2) are thus higher in Model A compared to Model B. The inaccuracy of the approximation of using homogenous polarizable continuum model decreases as the size of the model grows. The further away from the active site the truncation is made, the better this approximation works. That is, when a large model of the active site is used, most of the polarization effects on the reactive parts are already explicitly included in the quantum calculations. Thus, addition of continuum solvation on top of the cluster results of Model B does not affect the results significantly (see Fig. 6).

Another important point is that the effect of continuum solvation on the potential energy curve saturates very quickly as a function of ε (compare e.g. the curves of $\varepsilon = 4$ and $\varepsilon = 80$ in Fig. 3), which makes the particular choice of the dielectric constant less critical.

An important advantage of relatively small active site models is that the computational cost is much cheaper. This allows for the treatment of the system at higher level of theory, which is essential to obtain more reliable energetics. Also, smaller models suffer to a much lesser extent from multiple minima problems. With Model A, it is relatively easy to visually inspect whether the stationary points are in the same local minima with respect to the parts that are not participating in the reaction, something that is very hard to control in larger models, such as Model B. Finally, systematic build-up of models from smaller to larger allows for the identification of important groups and factors contributing the reaction characteristics, which is essential to gain deeper understanding.

Acknowledgments

We gratefully acknowledge financial help from: The Swedish Research Council, The Wenner-Gren Foundations, The Carl Trygger Foundation, and The Magn Bergvall Foundation.

Appendix A. Supplementary data

Supplementary data associated with this article can be found, in the online version, at doi:10.1016/j.bioorg.2007.08.003.

References

[1] S. Harayama, M. Rekik, K.-L. Ngai, N. Ornston, J. Bacteriol. 171 (1989) 6251.
[2] S. Harayama, M. Rekik, J. Biol. Chem. 264 (1989) 15328.
[3] L.H. Chen, G.L. Kenyon, F. Curtin, S. Harayama, M.E. Bembenek, G. Hajipour, C.P. Whitman, J. Biol. Chem. 267 (1992) 17716.
[4] H.S. Subramanya, D.I. Roper, Z. Dauter, E.J. Dodson, G.J. Davies, K.S. Wilson, D.B. Wigley, Biochemistry 35 (1996) 792.
[5] A.B. Taylor, R.M. Czerwinski, W.H. Johnson Jr., C.P. Whitman, M.L. Hackert, Biochemistry 37 (1998) 14692.
[6] R.M. Czerwinski, T.K. Harris, M.A. Massiah, A.S. Mildvan, C.P. Whitman, Biochemistry 40 (2001) 1984.
[7] M.C. Fitzgerald, I. Chernushevich, K.G. Standing, C.P. Whitman, S.B.H. Kent, Proc. Natl. Acad. Sci. USA. 93 (1996) 6851.
[8] J.T. Stivers, C. Abeygunawardana, A.S. Mildvan, G. Hajipour, C.P. Whitman, L.H. Chen, Biochemistry 35 (1996) 803.
[9] J.T. Stivers, C. Abeygunawardana, A.S. Mildvan, G. Hajipour, C.P. Whitman, Biochemistry 35 (1996) 814.
[10] W.H. Johnson Jr., R.M. Czerwinski, M.C. Fitzgerald, C.P. Whitman, Biochemistry 36 (1997) 15724.
[11] R.M. Czerwinski, W.H. Johnson Jr., C.P. Whitman, T.K. Harris, C. Abeygunawardana, A.S. Mildvan, Biochemistry 36 (1997) 14551.
[12] T.A. Soares, D.S. Goodsell, J.M. Briggs, R. Ferreira, A. Olson, J. Biopolymers 50 (1999) 319.
[13] G.A. Cisneros, H. Liu, Y. Zhang, W. Yang, J. Am. Chem. Soc. 125 (2003) 10384.
[14] G.A. Cisneros, M. Wang, P. Silinski, M.C. Fitzgerald, W. Yang, Biochemistry 43 (2004) 6885.
[15] G.A. Cisneros, M. Wang, P. Silinski, M.C. Fitzgerald, W. Yang, J. Phys. Chem. A. 110 (2006) 700.
[16] T.K. Harris, R.M. Czerwinski, W.H. Johnson Jr., P.M. Legler, C. Abeygunawardana, M.A. Massiah, J.T. Stivers, C.P. Whitman, A.S. Mildvan, Biochemistry 38 (1999) 12343.

[17] R.M. Czerwinski, T.K. Harris, W.H. Johnson Jr., P.M. Legler, J.T. Stivers, A.S. Mildvan, C.P. Whitman, Biochemistry 38 (1999) 12358.
[18] (a) N. Metanis, A. Brik, P.E. Dawson, E. Keinan, J. Am. Chem. Soc. 126 (2004) 12726;
(b) N. Metanis, E. Keinan, P.E. Dawson, J. Am. Chem. Soc. 127 (2005) 5862.
[19] C.P. Whitman, Arch. Biochem. Biophys. 402 (2002) 1.
[20] K. Tuttle, E. Keinan, W. Thiel, J. Phys. Chem. B 110 (2006) 19685.
[21] K. Tuttle, W. Thiel, J. Phys. Chem. B 111 (2007) 7665.
[22] (a) P.E.M. Siegbahn, Quart. Rev. Biophys. 36 (2003) 91;
(b) F. Himo, P.E.M. Siegbahn, Chem. Rev. 103 (2003) 2421;
(c) L. Noodleman, T. Lovell, W.-G. Han, J. Li, F. Himo, Chem. Rev. 104 (2004) 459;
(d) F. Himo, Theor. Chem. Acc. 116 (2006) 232.
[23] (a) C. Lee, W. Yang, R.G. Parr, Phys. Rev. B 37 (1988) 785;
(b) A.D. Becke, Phys. Review. A 38 (1988) 3098;
(c) A.D. Becke, J. Chem. Phys. 96 (1992) 2155;
(d) A.D. Becke, J. Chem. Phys. 97 (1992) 9173;
(e) A.D. Becke, J. Chem. Phys. 98 (1993) 5648.
[24] Gaussian 03 (Revision C.02), Frisch, M.J. et al., Gaussian, Inc., Wallingford CT, 2004.
[25] (a) V. Barone, M. Cossi, J. Phys. Chem. A 102 (1998) 1995;
(b) R. Cammi, B. Mennucci, J. Tomasi, J. Phys. Chem. A 103 (1999) 9100;
(c) A. Klamt, G. Schüürmann, J. Chem. Soc. Perkin. Trans. 2 (1993) 799;
(d) J. Tomasi, B. Mennucci, R. Cammi, Chem. Rev. 105 (2005) 2999.